

# Mean Field methods

Jacopo Cocomello, Antonio Anna Mele, Luca Zuanazzi

April 2020

# Introduction

We want to study the ground state of a system composed by  $N$  ultracold atoms trapped in an harmonic potential. If the atoms are bosons, by a mean field approximation we assume the ground state to be a product of single particle states

$$\Psi(\mathbf{r}_1, \dots, \mathbf{r}_N) = \prod_{i=1}^N \phi(\mathbf{r}_i) \quad (1)$$

From the variational principle it can be deduced that the best product of single particle states, that is the one that minimizes the energy functional  $\langle \Psi | H | \Psi \rangle$ , is the one made by the solution of the Hartree equation. As external and interacting potential we consider

$$V_{ext}(\mathbf{r}) = \frac{1}{2}m\omega^2 r^2 \quad V_{int}(\mathbf{r} - \mathbf{r}') = \frac{4\pi\hbar^2}{m}a\delta(\mathbf{r} - \mathbf{r}') \quad (2)$$

with the parameter  $a$  being typically called *scattering length*. Once inserted in Hartree equation, these potentials lead to the Gross-Pitaevskii equation for the radial part of the single particle wave function

$$\left( -\frac{1}{2} \frac{d^2}{dr^2} + \frac{1}{2}r^2 + Na\frac{u^2}{r^2} \right) u = \mu u \quad (3)$$

where  $\phi(\mathbf{r}) = r^{-1}u(r)Y_{00}(\Omega)$ . Notice that a change of units has been made so that now lengths are in unit of  $\sqrt{\hbar/m\omega}$  while energies are in unit of  $\hbar\omega$ .

A self-consistent procedure to solve (3) is to consider it as a standard Schrödinger equation with a potential  $v = \frac{1}{2}r^2 + Na\frac{\rho}{r^2}$ . Starting from a reasonable function  $\rho_0$ , we use Numerov's method or the finite-difference method to iteratively solve the equation

$$\left( -\frac{1}{2} \frac{d^2}{dr^2} + \frac{1}{2}r^2 + Na\frac{\rho_{i-1}}{r^2} \right) u_i = \mu_i u_i \quad (4)$$

each time updating  $\rho$  with the recursive definition  $\rho_i = \alpha u_i^2 + (1 - \alpha)\rho_{i-1}$ . Notice that, with this definition, any normalization condition imposed on  $\rho_0$  and  $u_i^2$  is automatically inherited by  $\rho_i$ .

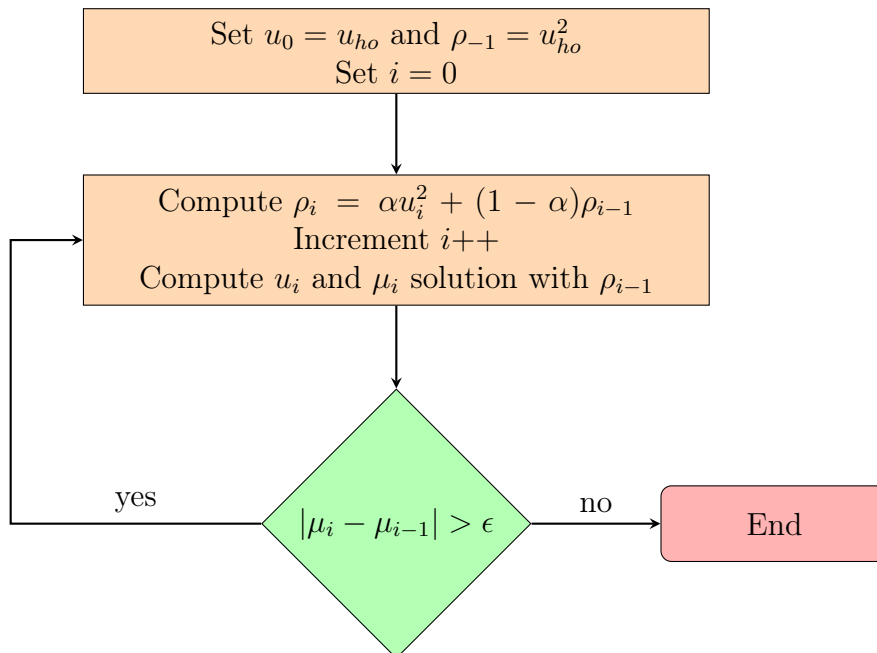


**Figure 1:** Flowchart of the self-consistent procedure.

For example, to construct  $\rho_0$ , we can use the ground state of the only harmonic part of the potential

$$u_{ho} = \frac{2r}{\pi^{1/4}} e^{-r^2/2} \quad (5)$$

In Figure 1 we show a flowchart of this iterative procedure, as ending condition we have chosen the convergence of the eigenvalue  $\mu$  within a certain precision dictated by the parameter  $\epsilon$ . The reason to not use only one previous solution to construct the potential (that is setting  $\alpha = 1$ ) is because in this way the procedure keeps alternating between two types of wave functions, one like the harmonic oscillator ground state  $u_0$  and the other peaked to some positive value of  $r$  like  $u_1$ , without never converging. This can be seen from Figure 2 where we plot, for the first 100 iterations, the solutions  $r^{-1}u_i$  and their respective potentials  $v_i = \frac{1}{2}r^2 + \frac{Na}{r^2}\rho_{i-1}$  for  $Na = 10$  and  $\alpha = 1$ .

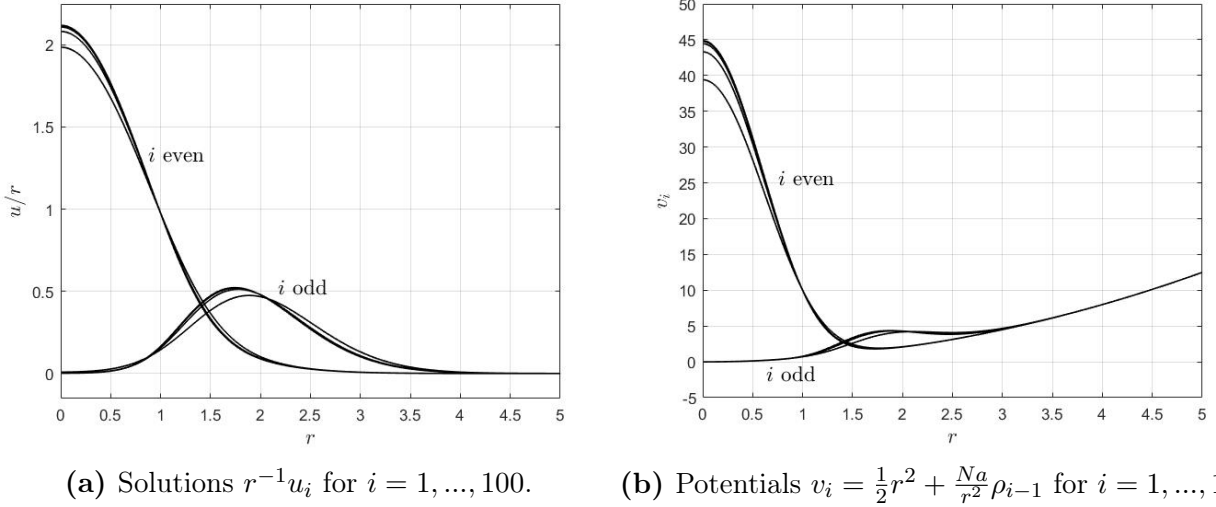


**Figure 2:** Solutions and potentials for  $Na = 10$  and  $\alpha = 1$  obtained with Numerov's method.

The problem can be solved setting  $\alpha \ll 1$ , as it can be seen from Figure 3a where we plot  $u_2$ , the first  $\alpha$ -dependent solution, for different values of  $\alpha$ . In this way the potential slowly changes from the  $i$ -even shape to a middle ground with the  $i$ -odd shape.

In Figure 3b instead we show the convergence of the procedure for the case of  $Na = 10$  and  $\alpha = 0.1$ .

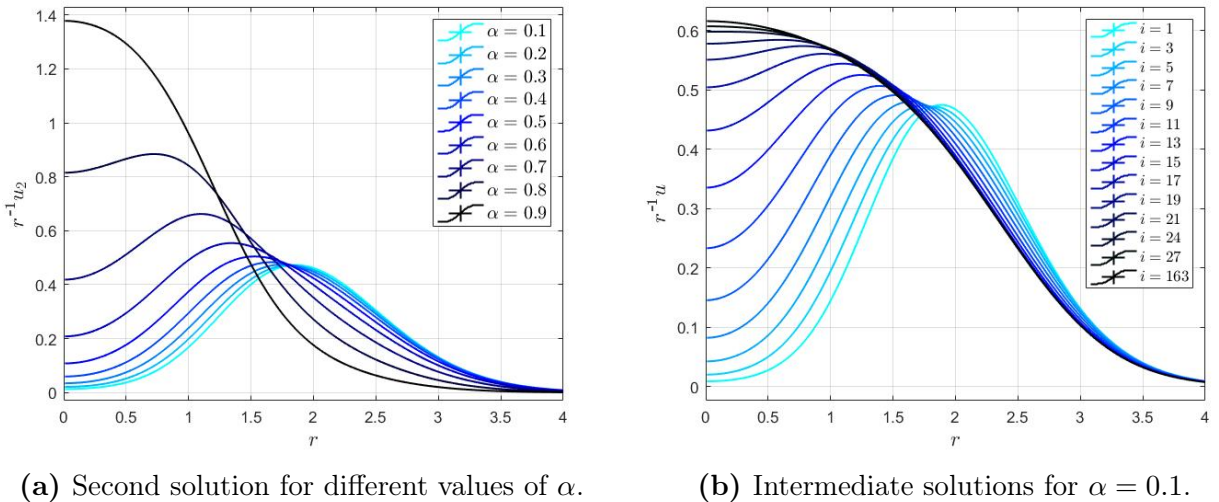


**Figure 3:** Eigenstates of the G-P equation for  $Na = 10$  obtained with Numerov's method.

The mixing process affects our solution through the parameter  $Na$ . On a physical ground this parameter sets the density of our system; therefore the contact interaction is more influent in the highly dense regime, rather than in the dilute limit. Our interaction potential changes at every iteration of the algorithm as a function of the eigenstate calculated at the previous step in the self-consistent mixing procedure. This happens for every dilute-wise system, but the actual change in the potential is weighted by the density of the system, as only the interaction potential is proportional to  $Na$  while the external harmonic part is constant at every iteration. Convergence of highly diluted systems, that is the limit  $Na \rightarrow 0$ , only involves the search for the correct shape of the eigenstate which satisfies the appropriate eigenvalue/energy condition. On the contrary, as diluteness decreases, the search for the correct eigenfunction is strongly influenced by previous (intermediate) solutions which dominate in the potential. We then understand that the value of the parameter  $\alpha$ , which governs the mixing procedure, becomes more important in the convergence of the solution as the value of the parameter  $Na$  increases, i. e. as the system becomes denser.

Another possible convergence criterion is a check on the energy per particle of the system. This quantity can be obtained through a direct evaluation of the energy per particle functional

$$E[\phi(\mathbf{r})] = \frac{\langle \Psi | H | \Psi \rangle}{N} = T[\phi(\mathbf{r})] + V_{ext}[\phi(\mathbf{r})] + V_{int}[\phi(\mathbf{r})] \quad (6)$$

or from the eigenvalue  $\mu$ . The relation between the eigenvalue and the energy per particle is obtained by projecting the equation (3) onto the same eigenstate  $\phi(\mathbf{r})$  from the left. This means in practice to multiply (3) by  $\phi^*(\mathbf{r})$  on the left and then integrate in coordinate space. If  $\phi(\mathbf{r})$  is a solution to the Gross-Pitaevskii equation it then must satisfy also the following relation

$$T[\phi(\mathbf{r})] + V_{ext}[\phi(\mathbf{r})] + 2V_{int}[\phi(\mathbf{r})] = \mu \quad \implies \quad E[\phi(\mathbf{r})] = \mu - V_{int}[\phi(\mathbf{r})] \quad (7)$$

Hence, as convergence condition we can choose  $|E[\phi(\mathbf{r})] + V_{int}[\phi(\mathbf{r})] - \mu| < \epsilon$ .

Such to implement this condition we have to calculate three integrals. Some considerations are necessary about the implementation of these calculations. At first we notice that the problem is spherically symmetric, then each functional is really a functional of the radial part of  $\phi(\mathbf{r})$ , which can be further worked out such that the functionals only depend on the  $u(r)$  part of the wave function. They can be defined in an operational way through this equation

$$T[\phi_i(\mathbf{r})] + V_{ext}[\phi_i(\mathbf{r})] + 2V_{int}[\phi_i(\mathbf{r})] = -\frac{1}{2} \int u_i \frac{d^2 u_i}{dr^2} dr + \frac{1}{2} \int r^2 u_i^2 dr + Na \int \frac{u_i^4}{r^2} dr. \quad (8)$$

Such to not introduce more approximations to our calculations, we evaluate the second derivative in the kinetic energy functional not by implementing a numerical approximation of the derivative but we rather make use of already at our disposal informations, i.e. the differential equation (4). This can be rewritten in the form

$$\frac{d^2 u_i}{dr^2} = \left( r^2 + 2Na \frac{\rho_{i-1}}{r^2} - 2\mu_i \right) u_i, \quad (9)$$

so that the convergence criterion becomes

$$\left| -\frac{1}{2} \int \left( r^2 + 2Na \frac{\rho_{i-1}}{r^2} - 2\mu_i \right) u_i^2 dr + \frac{1}{2} \int r^2 u_i^2 dr + Na \int \frac{u_i^4}{r^2} dr - \mu_i \right| < \epsilon. \quad (10)$$

Rearranging terms and recalling that  $\int u_i^2 dr = 1$ , this condition simplifies to

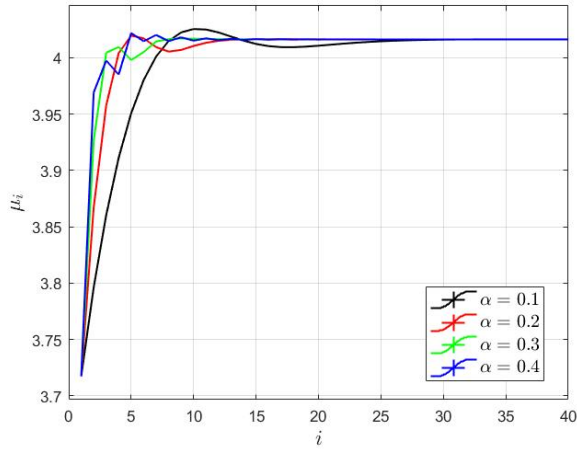
$$\gamma_i = \left| Na \int \frac{u_i^2}{r^2} (u_i^2 - \rho_{i-1}) dr \right| < \epsilon \quad (11)$$

such integral will be performed numerically with the trapezoidal rule. It cannot be more explicit than in this last expression that the density of the system is directly proportional to the difficulty of convergence. Note that, during the self-consistent procedure, when the convergence condition is not satisfied, the total energy per particle must be calculated through the following expression

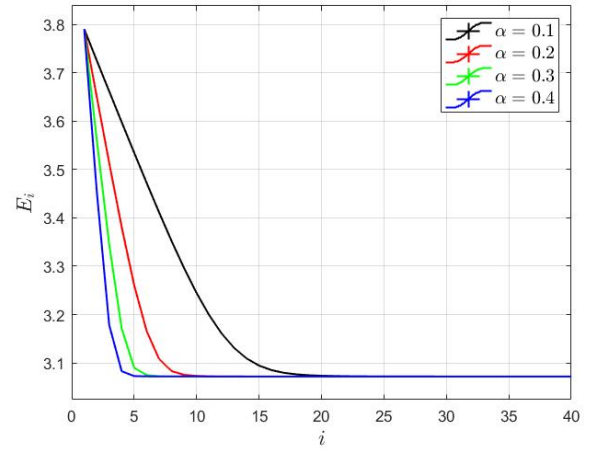
$$E = \mu + Na \int \frac{u_i^2}{r^2} \left( \frac{u_i^2}{2} - \rho_{i-1} \right) dr \quad (12)$$

## Numerov's results

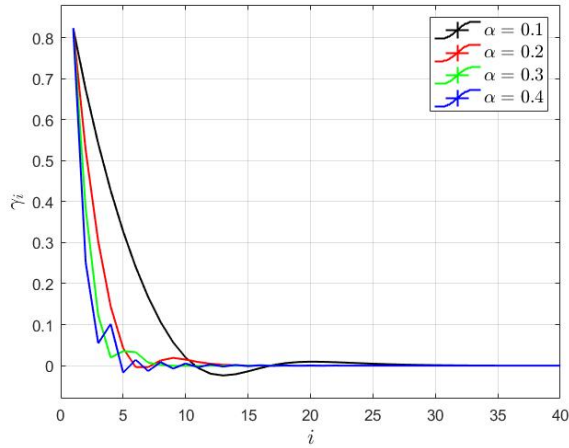
We start solving the Gross-Pitaevskii equation with Numerov's method for  $Na = 10$ . The results are shown in Figure 4.



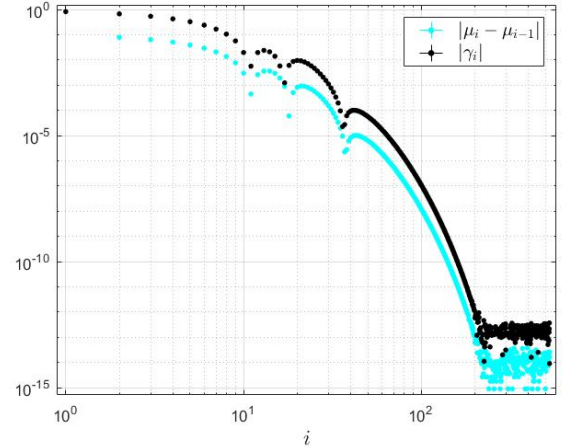
(a) Convergence of  $\mu$  for different values of  $\alpha$ .



(b) Convergence of  $E$  for different values of  $\alpha$ .



(c) Convergence of  $\gamma$  for different values of  $\alpha$ .



(d) Comparison of convergence criteria for  $\alpha = 0.1$ .

**Figure 4:** Solutions of the G-P equation for  $Na = 10$  obtained with Numerov's method.

We remark that the procedure does not converge for  $\alpha = 0.5$ . From Figures 4a and 4c, it may seem that the two convergence criteria are connected by a simple linear transformation. Indeed, in Figure 4d, we can see that the only difference is in a multiplicative factor of 10 (resulting in an additional constant of 1 decade in the log-log plot). This also means that the convergence of  $\gamma$  is a stronger condition, as it requires more steps than the convergence of  $\mu$ . For example, setting  $\epsilon = 10^{-10}$ ,  $\mu$  converges at the 141-th iteration while  $\gamma$  takes 19 more steps.

To be sure that the procedure converges to the same value for all  $\alpha$  in Figure 5 we plot some details of the convergence of the total energy per particle.

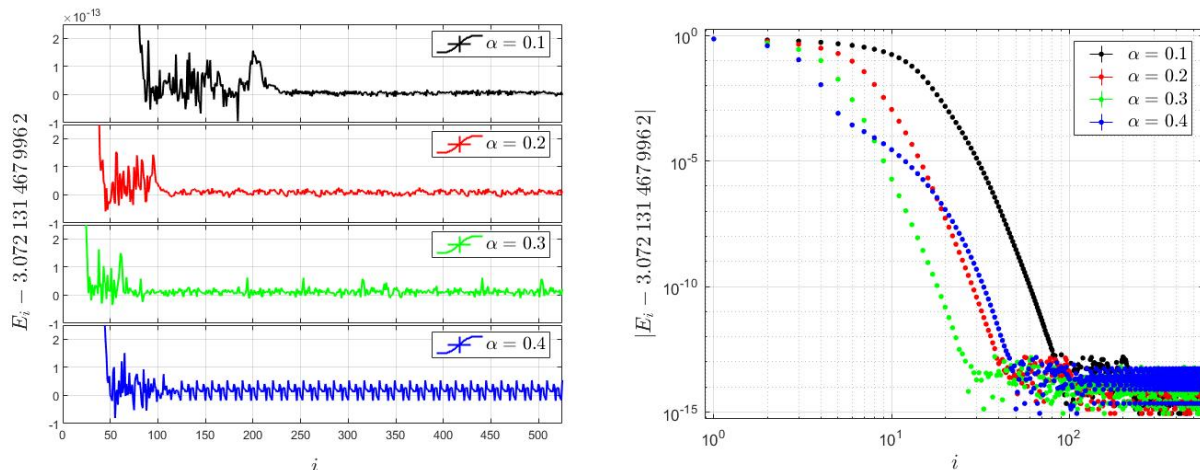


**Figure 5:** Details of the convergence of  $E$  for different values of  $\alpha$ .

In the first plot we can see that for  $\alpha = 0.4$  the energy shows small periodic oscillations for  $i \gtrsim 130$ ; this means that the procedure started alternating between a set of solutions. From the second plot instead we see that the value  $\alpha = 0.3$  gives the fastest convergence. Notice that, once the energy has converged, there are two regions with different numerical noise; for example, for  $\alpha = 0.1$ , the noise is more intense for the iterations  $80 \lesssim i \lesssim 210$ , and it later decreases of about one order of magnitude. We recognize that, the point where the noise decreases coincides to the point where  $\mu$  and  $\gamma$  converge and start showing numerical oscillations.

In order to check in a quantitatively way that the energy converges always to the same value, we calculate the mean and standard deviation of the energy when only the numerical noise is left, obtaining

$\alpha$	$E$
0.1	3.072 131 467 996 206(6)
0.2	3.072 131 467 996 208(7)
0.3	3.072 131 467 996 21(1)
0.4	3.072 131 467 996 22(2)

**Table 1:** Energy per particle for  $Na = 10$  and different values of  $\alpha$ .

We are now ready to vary  $Na$ . We repeat a similar analysis to the one made for  $Na = 10$  for different values of the density, obtaining

$Na$	$E$
0.01	1.503 975 260 360 2
0.1	1.538 560 942 328 4
1	1.811 218 038 800 1
10	3.072 131 467 996 2
100	6.874 919 663 029 8

**Table 2:** Energy per particle for different densities of the system.

Here there is an important problem to discuss: in the dense regime of  $Na = 100$  the initial harmonic ground state generates a high potential for small  $r$  which can dominate over the

harmonic potential at big  $r$  if the Numerov's method is not implemented carefully. This would imply to considerably increase the interval over which the solution is calculated with a subsequent increase of the computational time. To avoid this problem we preferred to change the algorithm described in the flowchart setting  $\rho_{-1} = 0$ . Looking back at Figure 2b, this means to slowly change the potential from an odd-like shape to a middle ground with the even shape, instead of starting from the even-like shape. The reason for which we didn't use this method right from the beginning is because now  $\rho_i$  is not normalized. Indeed it is easy to obtain

$$\int_0^\infty \rho_i(r) dr = 1 - (1 - \alpha)^{i+1} \quad i = -1, 0, 1, \dots \quad (13)$$

Therefore we have to make sure the self-consistent procedure worked *enough* iterations to neglect the error in the normalization of  $\rho$ . For example, if we use  $\alpha = 0.05$  after 600 steps the error in the norm is  $(1 - 0.05)^{601} \simeq 4 \times 10^{-14}$ .

In the end, we plot in Figure 6 the wave functions obtained for the different densities along with the convergence criterion  $\gamma$ .

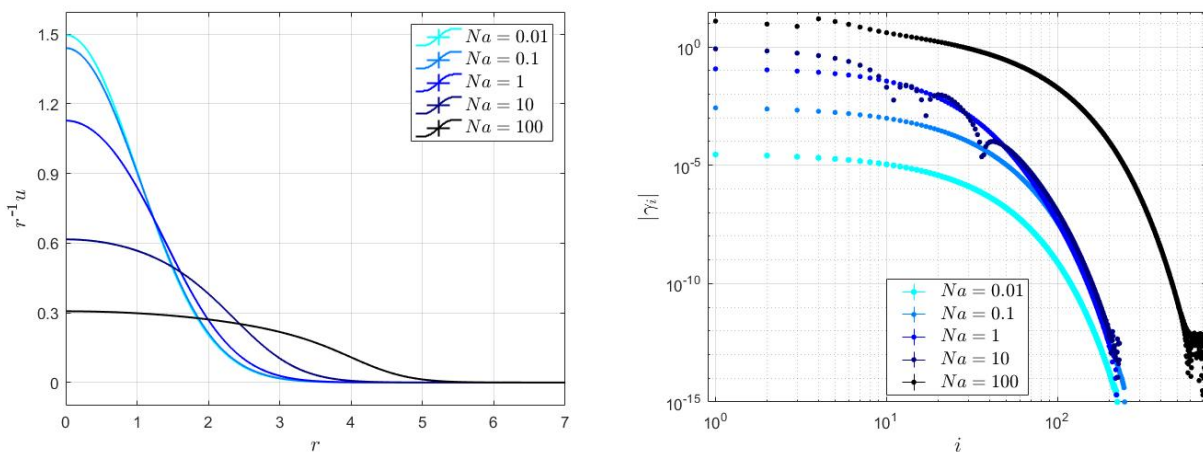


**Figure 6:** Solutions of the G-P equation for different values of  $Na$ . We used  $\alpha = 0.1$  except for the case with  $Na = 100$  for which we used  $\alpha = 0.05$ .

## Finite difference method

We want to solve G-P equation using the finite difference method. We begin defining a mesh of  $n$  points in the interval  $[0, r_{\max}]$ . The mesh is regular, with spacing  $h = r_{\max}/n$ . For brevity we define  $r_i = ih$  and  $u_i = u(r_i)$ .

We begin with the approximation of the second derivative of  $u$ , which appears in eq(3), with a three-point formula at a generic point  $r_i$  :

$$-\frac{1}{2} \frac{u_{i+1} - 2u_i + u_{i-1}}{h^2} + \frac{1}{2} r_i^2 u_i + Na \frac{\rho_{k-1,i}}{r_i^2} u_i = \mu u_i \quad (14)$$

where  $\rho_k = \alpha u_k^2 + (1 - \alpha)\rho_{k-1}$  (we need to use this effective function for the reasons explained in the previous section where the notation we are using is clarified). We can solve the equation iteratively, following the instructions in the flowchart (Figure 1).

This expression can be recast into an eigenvalues problem. We define

$$U_i = \frac{1}{h^2} + \frac{1}{2} r_i^2 + Na \frac{\rho_{k-1,i}}{r_i^2}, \quad (15)$$

therefore, we can write

$$\begin{pmatrix} U_1 & -\frac{1}{2h^2} & 0 & \cdots & \cdots & \cdots & 0 \\ -\frac{1}{2h^2} & U_2 & -\frac{1}{2h^2} & 0 & \cdots & \cdots & 0 \\ 0 & -\frac{1}{2h^2} & U_3 & -\frac{1}{2h^2} & 0 & \cdots & 0 \\ \vdots & & \ddots & \ddots & \ddots & & \vdots \\ \vdots & & & \ddots & \ddots & \ddots & \vdots \\ 0 & \cdots & \cdots & 0 & -\frac{1}{2h^2} & U_{n-2} & -\frac{1}{2h^2} \\ 0 & \cdots & \cdots & \cdots & 0 & -\frac{1}{2h^2} & U_{n-1} \end{pmatrix} \begin{pmatrix} u_1 \\ u_2 \\ u_3 \\ \vdots \\ \vdots \\ u_{n-1} \end{pmatrix} = \mu \begin{pmatrix} u_1 \\ u_2 \\ u_3 \\ \vdots \\ \vdots \\ u_{n-1} \end{pmatrix} \quad (16)$$

Notice that we assumed that  $u_0 = u_n = 0$ , thus the corresponding rows are missing and we have to consider an  $(n-1)$ -matrix. The diagonalization can be performed using the GSL subroutines from which we can obtain ground energy and the corresponding state. We can stop the iteration using one of the two different convergence criterions: the one with eigenvalues and the one which involves the energy computed from the functional. In Figure 7 we show the convergence of the procedure for the case of Numerov algorithm and for finite difference method with  $Na = 1$  and  $\alpha = 0.1$ .

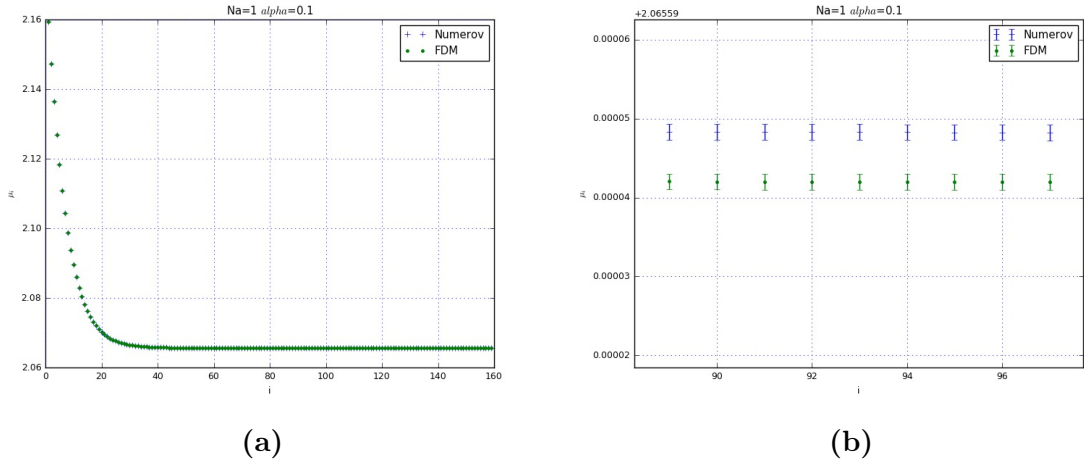


**Figure 7:** Eigenvalue  $\mu_i$  for each  $i$ -iteration with  $Na = 1$ ,  $\alpha = 1$  obtained with Numerov's and FDM method .

From figure 7 it is evident that the eigenvalue returned by the two methods is generally different for a factor (in this case  $< 10^{-5}$ ) depending by the problem parameters and by the chosen convergence criterion.

In order to compare the accuracy and execution speed between Numerov and finite difference method we consider the energy convergence criterion. The accuracy we obtain computing the ground energy is the same using both methods. The execution speed (computed using `time.h` routines) of the algorithm with Numerov is higher than the one with finite difference method. This is due to the fact that in the latter we need to perform matrix diagonalizations for each iteration, which typically require a great amount of operations. In table 3 there are the obtained results to compare the two methods.

$Na$	$E_{\text{Numerov}}$	$T_{\text{Numerov}} [s]$	$E_{\text{FiniteDifference}}$	$T_{\text{FiniteDifference}} [s]$
0.01	1.50397526036	0.8185	1.50395977394	48.22
0.1	1.53856094232	0.9571	1.53854656214	59.48
1	1.81121803880	1.208	1.81120874952	61.72
10	3.07213146799	5.594	3.07212758716	147.5

**Table 3:** Energy computed using Numerov’s and finite difference methods for different values of  $Na$ , with  $\alpha = 0.4$ ,  $h = 0.01$ ,  $n = 700$ .

In table 3, digits are reported within the energy error, accuracy is  $\epsilon = 10^{-11}$  for both methods using the above parameters; furthermore, we can observe that in all cases of  $Na$  the two methods return the same results until the fourth decimal digit.

As expected from eq. (11), we can observe that the execution time increase with  $Na$ .

## The case of attractive interactions

All the previous analysis was made considering a repulsive interaction between the atoms, i.e.  $a > 0$ . Now we consider attractive interaction and we want to understand up to which extent in the value of  $|Na|$  we can get a stable condensate.

We tried to manually change the value of this parameter among those used in the repulsive case: already for  $|Na| = 1$  the energy diverges to negative values. A more accurate analysis leads to state that stability is only ensured for  $Na \leq -0.574$ .

The stability of the attractive system is given by the interplay of the kinetic energy and the interaction contribution: the effective quantum pressure due to kinetic motion balances the collapsing effect that is created by attractive forces. This is true up to a certain critical value  $N_{cr}a$  beyond which attraction prevails and the condensate energy assumes indefinitely large negative values as it would be energetically favourable to acquire as much particles as possible. The critical value is reported in literature being  $N_{cr}|a| \approx 0.575$ .

It is quite natural to identify an instantaneous estimator of this balance for the systems the ratio of kinetic and interaction energy functionals

$$\frac{V_{int}[\phi_i(r)]}{T[\phi_i(r)]} = \frac{Na \int \frac{u_i^4}{r^2} dr}{\int \left( 2\mu_i - 2Na \frac{\rho_{i-1}}{r^2} - r^2 \right) u_i^2 dr}. \quad (17)$$

This quantity tends to be constant if the interplay between the two driving forces balances, i.e. if the condensate is stable, while it has a peculiar behaviour in the case of unstable systems.

In the following Figure 8 we show the behaviour of this estimator for values of  $Na$  in the neighbourhood of its critical value.

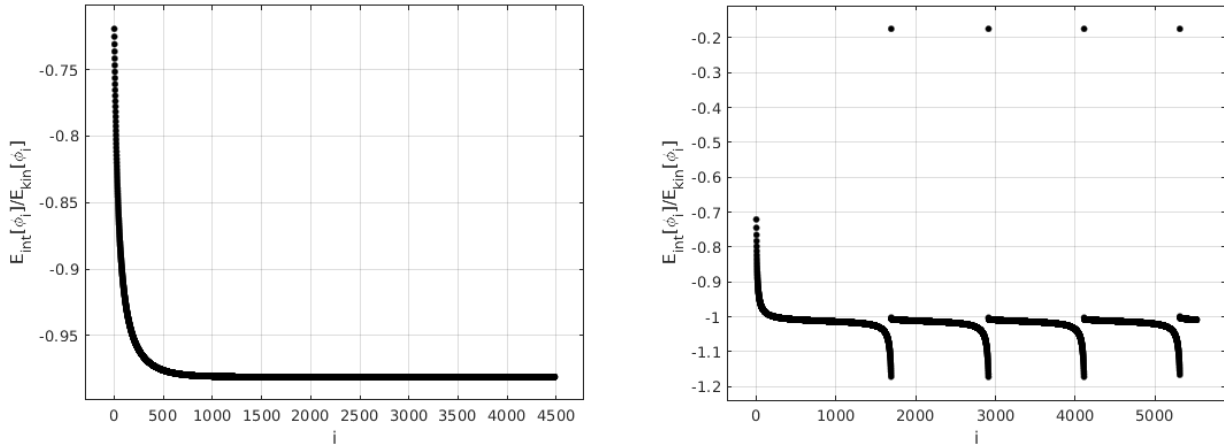


**Figure 8:** Behaviour of the local stability estimator for  $Na = -0.574$  on the left and  $Na = -0.575$  on the right. These graphs are obtained with  $\alpha = 0.4$ .

A qualitative difference in the shape of this functional is clearly perceivable as the parameter  $Na$  becomes lower than its critical value. This may be interpreted as a sign of physically unstable situation, though more accurate analysis should be carried out to better understand physical and computational criticalities in this regime.